e-ISSN: 2146 - 9067

International Journal of Automotive Engineering and Technologies

journal homepage:
https://dergipark.org.tr/en/pub/ijaet

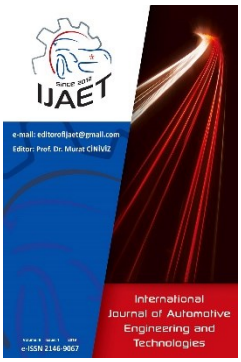

Original Research Article

Investigation of the effect of Cr_2O_3-2 % TiO_2 coating on braking performance

hosted by Turkish JournalPark ACADEMIC

İbrahim Mutlu[1], Bekir Güney[2,*], İbrahim Erkurt[3]

[1] Afyon Kocatepe Üniversitesi, Türkiye
[2] Karamanoğlu Mehmetbey Üniversitesi, Türkiye
[3] Afyon Kocatepe Üniversitesi, FBE, Türkiye

ARTICLE INFO

* Corresponding author
guneyb@kmu.edu.tr

Received: July 15, 2019
Accepted: Dec 23, 2019

Published by Editorial Board Members of IJAET

ABSTRACT

The brake discs of the new generation vehicles operate with very high speed and tough braking conditions. Therefore, high performance in braking is essential in terms of human and vehicle safety. In vehicles, the braking performance criterion is to control the speed of the vehicle safely without causing a mechanical failure. During a braking process in a moving vehicle, an excessive abrasion occurs. The aim of this study was to investigate the performance of the brake disc coated with Cr_2O_3-2%TiO_2 (Metco106F) composite powder by using the plasma coating method to increase the abrasion resistance of automobile brake disc. The braking test was performed according to the SAEJ2430 braking test standard. The microstructure, hardness, wear and braking performance characteristics of the coating were investigated. Our results showed that the coated disc exhibited better wear resistance than the uncoated disc under the different wear mechanisms at high temperatures. The obtained coefficient of friction revealed that the coated disc showed better braking performance.

Keywords: Ceramic Composite, Plasma Spray, Wear, Braking Performance

1. Introduction

The main components of the brake system consist of the brake disc and brake linings. Vehicles are designed to convert kinetic energy to friction energy by applying braking force. In particular, most of the braking are performed by the disc. Because of the heat energy generated during this process, the brake disc operates in a high temperature environment. Therefore, the frictional heat associated with braking increases the temperature in the disc and the lining, which greatly affects the life and performance of the brake disc [1, 2]. The brake disc is connected to the axle and rotates with the wheel. The brake system is required to press the lining on both sides of the disc in terms of occurring friction. A larger disc surface area exposed to air provides better heat dissipation. However, it is susceptible to frequent locking and braking weakening.

In high-speed vehicles, the brake disc subjected to braking force is subject to wear by the effect of the friction force between the disc and the lining. The abrasion and tear of the disc and

lining increases at high speeds compared to low speeds. In addition, braking efficiency is reduced due to increased temperature during braking [3,4]. Also, the life of the discs is reduced due to increased heat and braking. This may result in accidents due to disc breakage. Therefore, maintenance and use costs may increase [3-6].

Brake discs are usually made of gray cast iron due to their high damping capacity, good thermal conductivity and high strength [7]. The performance of the brake system in a vehicle is determined by the tribological characteristics of the friction pair consisting of a gray iron disc and lining [8]. The coefficient of friction must be relatively high and stable under all operating conditions such as temperature, humidity, speed, load and road condition. In addition, vibration absorption, long life, high comfort are other preferred features.

The surface properties of the brake disc exposed to high temperatures need to be improved. The most commonly used method for solving such problems arising from friction and wear mechanisms is coating the surfaces [9.]

Thermal spraying coatings method, which is one of the surface coating methods, can be applied quickly and practically, and have been widely used in a wide variety of applications to improve wear and corrosion properties. Plasma spraying technique, one of the most widely used thermal spraying methods, has been widely used technique for coating ceramic composite materials such as Cr_2O_3, Al_2O_3 or TiO_2 to metal components [10-14]. Ceramic coatings using atmospheric plasma spraying (APS) on the surfaces of metallic materials significantly improve the hardness, durability, abrasion and corrosion resistance of metal components through eliminating surface defects [15-17]. Without the use of plasma spray coating method, the most commonly used composites for perfect surface quality to host material are cermets such as Ni-SiC, Zn-ZrO_2, Cr_2O_3, Ni-Al2O_3, TiO_2, MgO, NiCrBSi, W_2C, WC-Co, WCCoCr, WC-Ni, WC-Cr_3C_2-Ni and Cr_3C_2-NiCr. Cr_2O_3 and TiO_2 ceramic composites show better wear, corrosion, oxidation, hardness, high temperature resistance and chemical stability properties [10-24]. Therefore, ceramic coatings are widely used in automotive, marine, industrial, aerospace and biomedical sectors which are more exposed to wear and corrosion [17].

In our previous study [10], we investigated the temperature-dependent properties of wear, friction and braking performances by coating the brake disc with Cr_2O_3-40%TiO_2 by plasma spray method. This work focuses on braking properties of a Cr_2O_3-2%TiO_2coated discs by plasma-spraying method and uncoated disc.

2. Materials and Methods

2.1. Materials preparation

The coated and uncoated discs are shown in Figure 1. The geometric properties of these discs used in the experiments are given in Table 1. The results of the spectral analysis of the gray cast iron sample (GG25) are given in Table 2.

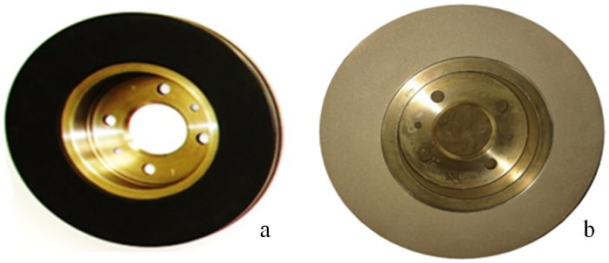

Figure 1. View of the brake discs used in this study
a) Uncoated disc, b) Coated disc

Table 1. Geometric properties of the disc used in this study

Disc specifications	Definition/Value
Disc diameter (mm)	280.00
Disc thickness (mm)	24.0
Minimum thickness (mm)	21.8
Disc type	Air ventilation brake disc
Disc surface	Standard
Number of bore	4
Hub diameter (mm)	100
Hub height (mm)	44.0
Central diameter (mm)	61.0
Inner diameter (mm)	140.0
Wheel bolt hole diameter (mm)	13.6

Table 2. The chemical composition of the uncoated disc sample

Elements	Wt.-%	Elements	Wt.-%
Fe	93.56	Mo	0.021
C	3.61	Ni	0.033
Si	1.81	Cu	0.005
Mn	0.586	Nb	0.000
P	0.025	Ti	0.015
S	0.023	Mg	0.003
Cr	0.116		

Two samples of brake linings used in this experimental study are shown in Figure 2. These

are commercial brake linings widely used in automobiles. They have a surface area of one inch^2, available on the after-market in accordance with SAE J661 under "Brake Lining Quality Control Test Procedure" [25].

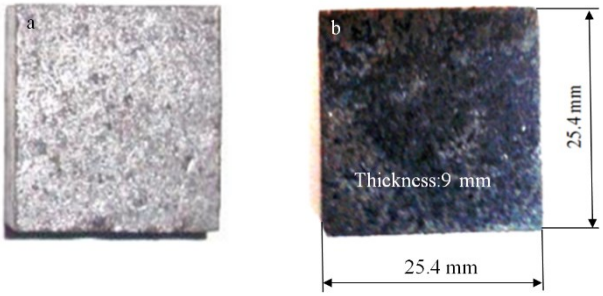

Figure 2. The images of the brake lining used in this study after the testing for a) Uncoated disc and b) Coated disc

2.2. Coating material properties

When chromium Cr_2O_3-2TiO_2 (Metco 106F) with grain size between 39 and 88 µm use as surface coating material, it provides a remarkable wear resistance, thermal deformation resistance under high temperatures, and corrosion resistance. In addition, it possesses high fracture toughness and maintains these characteristics up to 540 °C [26].

Cr_2O_3 is an important refractory material due to its high melting temperature (~ 2300 °C) and high temperature oxidation resistance [27]. These coatings are generally preferred in the fields where corrosion resistance, abrasive wear resistance, toughness, and ductility are of necessity [28]. Since it adheres well to the surface, it has high adhesion strength and high hardness value (2300 $HV_{0.5}$). As Cr_2O_3-2%TiO_2 coating produces such a high friction coefficient like 0.8, using it as a filling coating is possible [29].

In ceramic coatings made by plasma spraying, corrosion resistance increases with decreasing porosity, coating thickness and surface roughness [30].

2.3. Coating procedure

Sample surface was prepared by spraying SiC abrasive powder (35 grit). In order to obtain surface roughness in the best possible way, surface roughening procedure was conducted with 90° angle, under a pressure of 9 bar and at an average roughness value of Ra=8-9 µm with dry and clean air and sanding material. Chemical oil solvent materials were used to clean the surface from lubricants.

Atomized, metallic bonding coating Ni20Cr (Metco 43F-NS) powder with grain size between 11 and 53 µm was applied on the cast iron sample with the thickness of 30µm. During the Ni20Cr bonding coating application with plasma spray method with Ar+H_2 gasses, cooling with compressed air at a pressure of 3-5atm was conducted on the back of the sample in order to prevent overheating. Lamellar graphite cast iron sample was coated with the following plasma parameters in Table 3.

Table 3. Plasma spray parameters

Coating parameters	Specification/Value
Powder coater	Cr_2O_3-2%TiO_2
Substrate	GGL
Primary plasma gas (Ar) (l/min.)	44
Secondary plasma gas (H_2)(l/min)	15
Plasma current (A)	500
Plasma voltage (V)	60-70
Plasma gun type	METCO 3MB
Nozzle and electrode	W cathode-Cu anode
Nozzle diameter (mm)	8
Spraying distance (mm)	100
Injector angle	90°
Powder feed rate (g/min)	42
Powder carrier gas (Ar)(l/min)	6

2.4. Test configuration

The schematic configuration of the brake test device is shown in Figure 3. The brake test device was produced to provide the essentials of Dynamometer Effectiveness Characterization Test for Passenger Car and Light Truck Brake Friction Products/Brake Effectiveness Evaluation Procedure (SAE J2430/BEEP) developed by the Brake Manufacturers Council of North America (BMC). This device which was utilized to test the braking performance simulated the desired technical specifications from a single-disc dynamometer. The test results are shown in Figure 4. To carry out performance tests, a Windows based Delphi program was developed.

2.5. Experimental procedure

On the brake test device, the dry friction performance of the disc-brake lining couple was determined by factors such as instrument checks, burnish, effectiveness, fade, thermal performance, cooling down, recovery ramp, re-

burnish, second effectiveness and friction stability. The SAE J2430 test standard was chosen in order to fully examine the dry friction behavior [31-34].

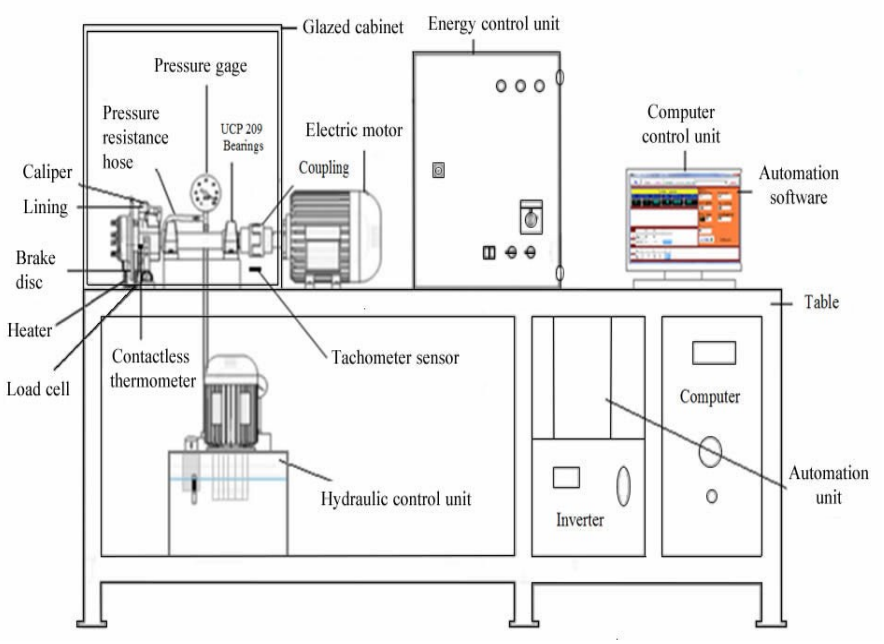

Figure 3. Schematic diagram of a brake dynamometer

A single-disc full-scale car inertia dynamometer was used in assessments of the braking performance. It was enclosed by a cabin in order not to affect the experimental setup by external air flow and to control the noise. An electric motor was used to run the setup. The test steps were listed in Table 4.

Table 4. Test procedure

1- Measurements before the experiment	surface roughness hardness weight
2- Main test steps of the experimental procedure (SAE J 2430)	Instrument check stop (23 cycles) Burnish (200 cycles) Effectiveness (16 cycles) Fade (15 cycles) Hot performance (2 cycles) Cooling (4 cycles) Recovery ramp (2 cycles) Reburnish (35 cycles) Final effectiveness (15 cycles)
3- Measurements after the experiment	surface roughness hardness weight

The test procedure steps were controlled with the computer program. Each type of brake lining and cast iron discs can be tested by the setup [35]. There were nine steps, the test duration was 14 hours, and the total number of cycles was 312. Full details of the test steps are obtained from SAE J 2430, and measurements obtained from the experiment were plotted in Figure 4.

3. Results and Discussion

3.1. Braking performance: coefficient of friction

Performance criteria of the uncoated disc and the coated disc with Cr_2O_3-2%TiO_2 powder were obtained from the brake testing device. Figures 4a and 4b show the results of instrument checks, burnish, effectiveness, fade, hot performance, cooling, recovery ramp, re-burnish, second effectiveness and friction stability. The general characteristic of coated disc was determined as an increase in temperature and the friction coefficient progressing approximately the same as the original disc.

The life of the brake discs depends on many different variables, such as the number of braking forces, the amount of braking force and the braking conditions. However, it is theoretically guaranteed to provide an average wear rate of 80.000-100.000 km or 10% in thickness reduction provided that it is continuously controlled by the manufacturers. The low wear of the discs and pads in the braking system not only ensures their long service life, but also contributes to the reduction of wear-related emissions. In this way, economic losses are prevented.

The coefficients of friction and temperatures depending on the normal force, contact pressure and velocities are also shown in Figures 4a and

4b. The structural integrity of the braking discs was tested with 312 braking cycles in total for 14 hours [31]. During the test, the highest temperatures in the uncoated disc and the coated disc measured by a non-contact thermometer were 294 °C and 365 °C, respectively.

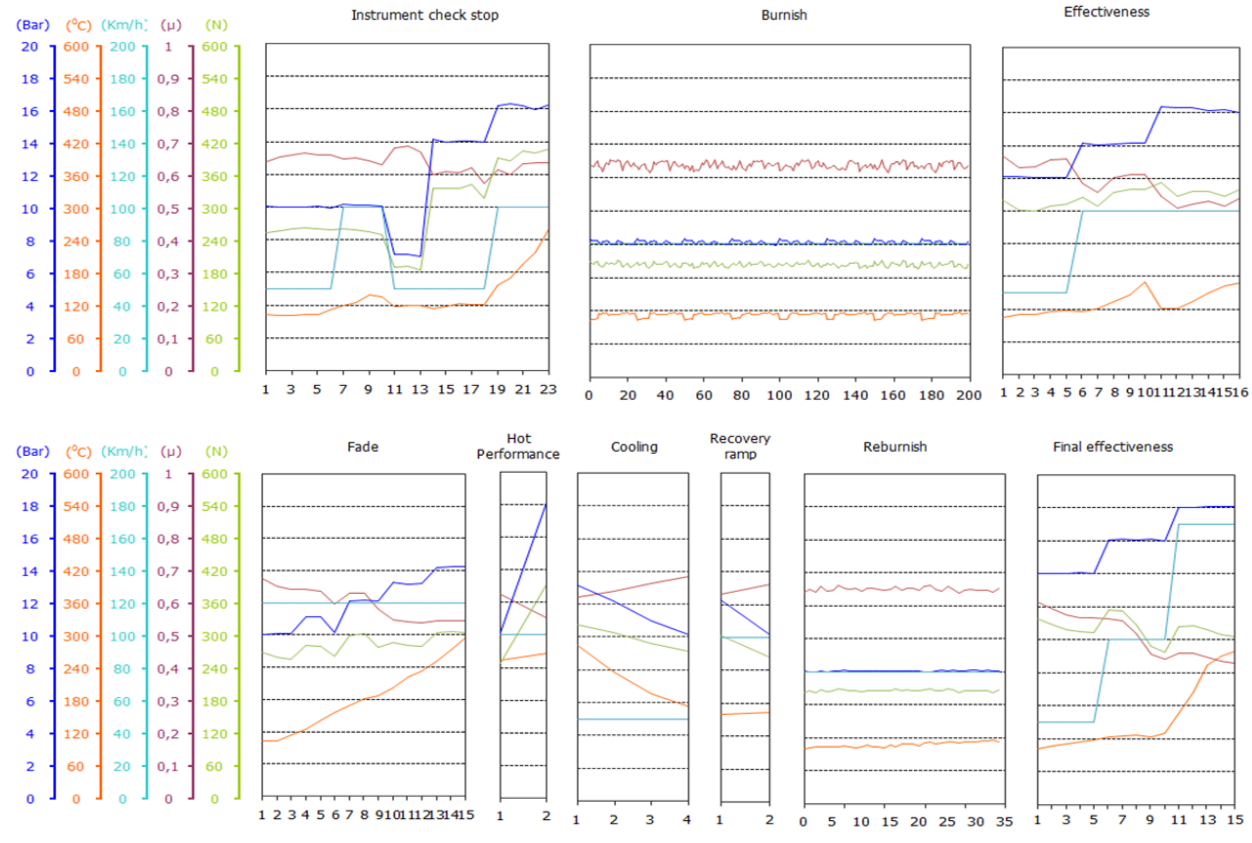

(a)

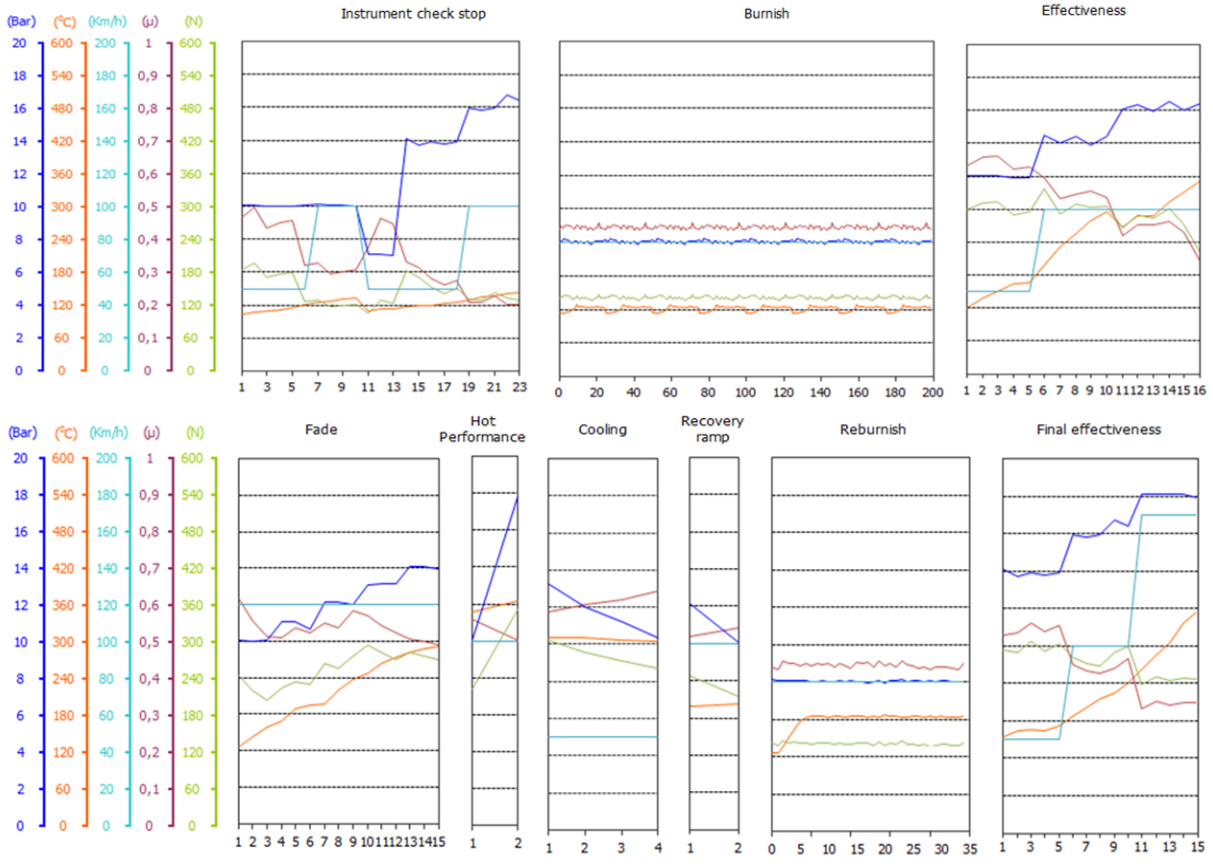

(b)

Figure 4. a) Characteristic data of uncoated brake disc, b) Characteristic data of Cr2O3-2%TiO2 coated brake disc

It was seen that the coefficient of friction of the coated disc decreased while braking force gradually increased [36]. When velocity and contact pressure increased at speed between 50-160 km/h, the coefficient of friction decreased [37]. As seen in Fig. 4a and 4b, when temperature increased, there was a decrease in the coefficient of friction of both discs in all effectiveness (such as fade, burnish, hot performance, and so on). This was due to physical and chemical changes in the friction surfaces of substrates [38].

As it is discussed previously [39], the microstructures of the disc–brake lining materials and their tribological properties are changed because of the effect of raising temperature at the disc-brake interface [40]. Moreover, a thin oxide layer or thermal film forms on the disc-brake lining friction interface. The coefficient of friction decreased at high temperatures due to oxide or thermal films protecting the disc against mechanic wear. However, this situation is not desired as it leads to less braking performance. The bigger is the difference in coefficient of friction of the cold and hot surfaced discs while in contact with the brake lining, the lower is the friction stability of contacting surfaces between brake lining and disc. For safe driving, it is desirable for this coefficient to be stable as well as high.

It can be seen from the Fig. 4a and 4b that the average coefficient of friction of the uncoated disc under high braking force with the effect of temperature was 0.59 at contact pressure of 18 bar and it was 0.53 for the coated disc. The average coefficient of friction of the uncoated disc with the cooling effect was 0.55, and it was 0.48 for the coated disc. The average coefficient of friction of the uncoated disc with the final effectiveness was 0.50, and it was 0.44 for the coated disc. All tests are agreement with SAE J 2430 [34]. When it is considered that the brake linings used were of GG class, Cr_2O_3-TiO_2 coating produced a high friction coefficient of 0.8 [29]. At the final effectiveness part, the friction coefficient receded from 0.63 to 0.44 due to a phenomenon defined as fade [8].

At different temperatures and contact pressures, the surface roughness affected the coefficient of friction, and therefore the wear rate decreased. The surface roughness of the coated disc was lower than that of the uncoated disc. According to SAE J2430/BEEP, criteria such as instrument checks, effectiveness, fade, thermal performance and final effectiveness are taken into account for a similar braking distance while evaluating braking performance.

In this study, uncoated disc and coated disc samples exhibited the coefficient of friction within the limits determined in standards under different conditions such as shear rate, pressure and temperature. The discs exhibited the ability to stop into limitations in the event that the maximum contact pressure of 18 bar was exerted on the pedal which led to about the normal load of 667 N, and that the surface temperature reached at the highest level. After the instrument check stop and in the final effectiveness tests, the coefficient of friction decreased linearly. These results satisfied BMC criteria, and it could be observed at 50, 100, and 160 km/h with a deceleration of 0.8 g.

3.2. Microstructures of rubbing surfaces

Microstructures of the uncoated disc and coated disc were examined by means of a light microscope (LM) and scanning electron microscopy (SEM), with energy dispersive spectrometry (EDS). By the thermal coating process, a surface microstructure was obtained with high abrasion resistance and better environmental performance (i.e. dust, humidity) [41]. Figure 5. shows images of typical gray iron microstructures containing graphite flakes, pearlite (ferrite and cementite layers), and free ferrite of the polished and etched (5%HNO_3 95%CH_3OH) cast iron brake disc.

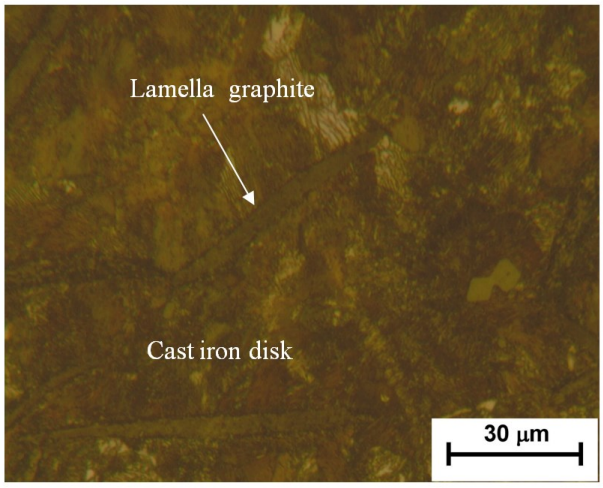

Figure 5. An example of image taken by a LM micrograph from the GGL sample surface at 30x magnification, showing porosity and lamella graphite

Ni20Cr bonding was used in order to eliminate

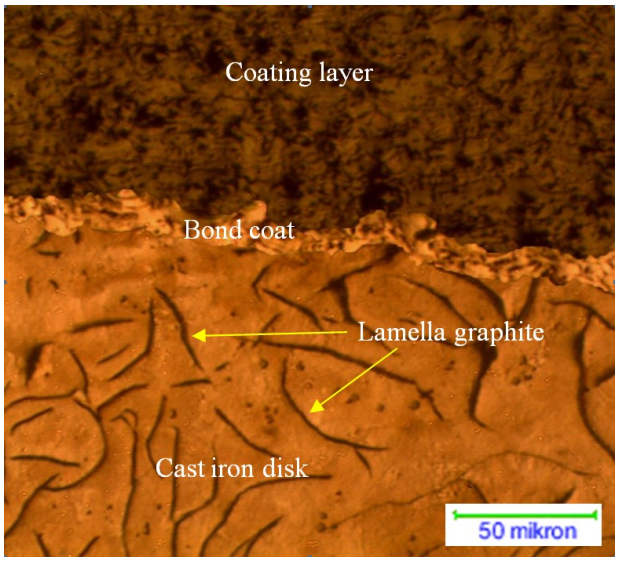

Figure 6. An example of image taken by LM micrograph from the cross-section of the coated sample at 50x magnification, showing coating layer, undercoat material and cast iron substrate

the incompatibility between metallic lamellar graphite cast iron sample and brittle, hard, and fragile coating material containing oxide structures. That the Ni element provided the formation of a tough and ductile structure is observed from the light microscope micrograph obtained from the coating cross-section in Figure 6.

Unmelted, partially melted, and completely melted areas are observed in the LM image in Figure 6. For the region near the coating boundary, the average porosity measured using the image analysis technique with ImageJ at 50x magnification is 2.41% compared to 4.91% at the upper region of the coating.

SEM image of the coated lamellar graphite cast iron sample is shown in Fig. 7. It is observed that a remarkable physical bond is created due to the fact that Ni element adapts itself to lamellar graphite cast iron material thanks to strong diffusion and that mechanical interaction is at the desired level. Similar to previous studies [10, 42-51], oxide composites within the coating layer, inclusion (Figure 7.) and the presence of a low amount of porosity were established with imaging analyses.

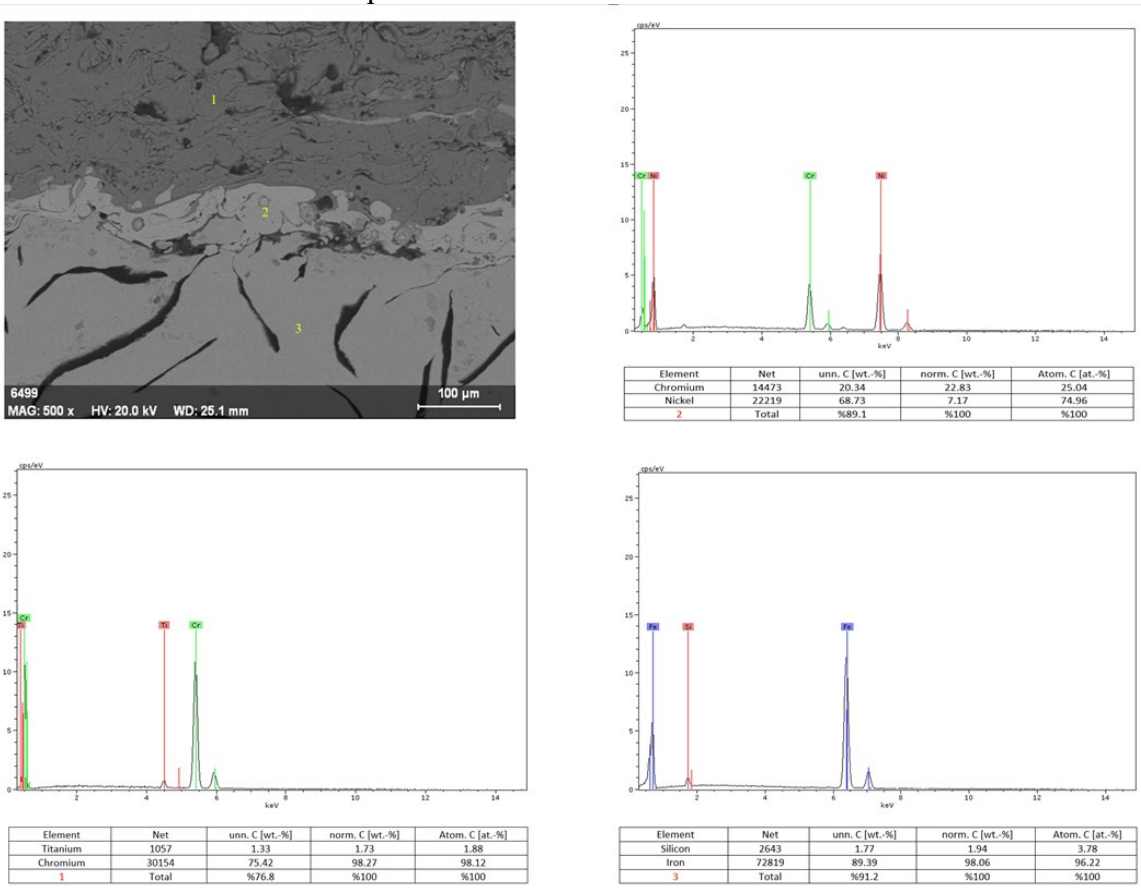

Figure 7. SEM micrograph (x100) taken from cross section of the disc coated with plasma spraying Cr_2O_3-2%TiO_2 and analysis of the points taken from SEM micrograph of cross section the disc coated

In addition, the amount of porosity changes depending on the surface porosity of lamellar graphite cast iron material, spray distance, temperature, and thickness of coating [11].

As noted in previous studies [42-44], a lamellar microstructure formed by molten metal droplets

hitting the substrate and constantly wetting it in thermal spray technique was observed in the micrograph shown in Figure 7, lamellar structure was formed by molten particles hitting substrate, being deformed, and solidifying [45]. These lamellar were composed parallel to substrate, and the midsections of lamellae were thick, and decrease the thickness in lamellae towards the ends [46].

Point 1 in Fig. 7 (a). was taken from the light gray region of the micrograph with 1000x magnification characterized by the section of coating named as Cr_2O_3-2%TiO_2 ceramic coating, and EDS analysis number 1 in Figure 7 demonstrates a microstructure rich in chromium. Spot 2 overlaps to a great extent with typical bonding NiCr elemental analyses in number 2 EDS analyses of the white region in Figure 7. Spot number 3 taken from the same micrograph demonstrates a microstructure rich in Si and Fe found as a result of EDS analysis number 3 in Figure 7.

In general, it is noted from the light microscope and SEM images that there was an excellent bonding resistance between coating layer, binding material, and lamellar graphite cast iron. Through the coating treatment, surface structures with high wear resistance and resistance to external factors were obtained.

3.3. Tribological performance

The hardness, wear, surface roughness, and the average values of the coefficient of friction were measured before and after braking tests of the uncoated disc and coated disc and brake linings. The results are given in Table 5.

Temperature increases due to the conversion of kinetic energy to heat during friction [8,53]. In addition, a very high temperature rise occurs on the friction surfaces, with increased load and braking time in braking process. The mechanical properties of the friction material are adversely affected by the effect of the temperature and the developing wear mechanisms. Contact configurations also change. A sudden increase in wear occurs at high temperatures [38]. The increase in temperature during brake application and the decrease in friction coefficient are called as friction attenuation, and friction attenuation at high temperatures is a critical feature for the materials used for friction [8].

Nowadays, basic information about the micro-sized contact on the interface of the disc, brake lining and the friction mechanisms is very limited. One of the most important factors affecting the coefficient of friction is the surface roughness. It has an effect on the amount of surface contact. The increase in real contact area means an increase in the numbers of junctions or micro-welds in the roughness plateaus depending on the sliding movement. The real contact areas in brakes in contact with disc surface have a great positive impact on the coefficient of friction [52].

The surface roughness values of the discs were measured by marking the disc surface with 10 equal parts from 10 sections before and after braking test. The average surface roughness (Ra) of the brake lining samples is measured by a profilometer (Table 5). The contacting surface layers due to dry friction became micro and macro pairs by smoothing. Although the surface roughness of the uncoated disc, which initially had a very high surface roughness, decreased from 1.515 µm to 0.354 µm during dry friction, the surface roughness of the coated disc increased from 0.302 µm to 0.694 µm due to the scratching of the coated disc surface caused by the brake lining. The uncoated disc with a lower roughness displays better braking performance by producing a higher coefficient of friction. As a result, the wear rate between the disc and brake lining reduced. Furthermore, the friction interface temperatures of the coated disc were lower than that of the interface of the uncoated disc. The coated disc displayed stability through delayed surface temperature.

The surface hardness of the uncoated disc and coated disc was measured with a micro-hardness tester. While the hardness of uncoated sample was measured as 258 HV, hardness of Cr_2O_3-2%TiO_2 coated sample was measured as 328 HV.

The hardness value of the coated disc is higher than the original disc due to the presence of oxidized hard phases in the coating structure. This high hardness also means that the coating has better wear resistance.

The wear depth and measurements of the mass loss of disc due to wear are given in Table 5. The mass loss was measured by a weighing machine with an accuracy of 0.1g. It can be seen that the variety of coefficient of friction exhibited by the

disc-brake lining materials in a braking system is not a sufficient result to evaluate the braking performance. Even if the coefficient of friction is high enough, change-over time of a short-lived disc-brake lining pairs create a significant disadvantage. In this situation, the wear rate which determines the disc and brake lining existence is as important as the coefficient of friction. In general, when the coefficient of friction increases, the wear rate also increases [53]. However, when both of the tribological and mechanical properties are evaluated together, the Cr_2O_3-2%TiO_2 coated disc exhibits a better tribological performance in terms of low wear rate and almost the same coefficient of friction.

Table 5. Tribological values of the uncoated disc and coated discs

Tribological properties of used discs	Uncoated disc	Coated disc
The roughness of the beginning surface of the disc (μm)	1.515	0.302
The roughness of the finishing surface of the disc (μm)	0.354	0.694
The roughness of the beginning surface of the brake lining (μm)	2.771	2.267
The roughness of the finishing surface of the brake lining (μm)	1.564	1.346
Hardness of the disc ($HV_{0.5}$)	258	328
Mass loss of the discs (g)	1.5	0.7
Mass loss of the brake lining (g)	9.557	7.931
Thickness reduction of the discs (mm)	0.031	0.008
Thickness reduction of the brake lining (mm)	6.294	5.231
The highest temperature of the disc (°C)	294	365
Coefficient of friction of the instrument checks (μ)	0.62	0.37
Coefficient of friction of the burnish (μ)	0.66	0.47
Coefficient of friction of the effectiveness (μ)	0.57	0.45
Coefficient of friction of the fade (μ)	0,60	0.55
Coefficient of friction of the hot performance (μ)	0,59	0.53
Coefficient of friction of the cooling (μ)	0.65	0.62
Coefficient of friction of the instrument recovery ramp (μ)	0.63	0.53
Coefficient of friction of the re-burnish (μ)	0.65	0.45
Coefficient of friction of the final effectiveness (μ)	0.50	0.44

Wear formation between two or more different materials is inevitable when in contact with different loads and speeds [55,56]. Both friction and wear are the result of tribological contact between two sliding surfaces at the same time [57,58]. In general, a wear mechanism ultimately leads to another wear and at the same time the combination of different wear mechanisms has a certain effect on the friction and wear properties of the material [55,56]. In ceramic coatings sprayed with plasma, porosity, imperfections, the interface between the particles serve as potential zones for a stress concentration at which the cracks can be nucleated [59-61]. Grain breakage is supported by the accumulation of plastic tension, displacement accumulation and thermal stresses at the grain boundaries [62]. This interaction damages the surface and substrates between the friction material and the counter material, resulting in shorter service life and even a degradation of the material [55,56]. In addition, as reported by Suzdal'tsev, the coated sample surface produced a relatively low coefficient of friction, causing low wear [63]. The way the material detaches from the surface depends on several wear mechanisms. In real contact, it is possible that more than one wear mechanism is effective at the same time. Therefore, the wear mechanism affects the worn surface morphology considerably. Moreover, comparative evaluation of the abrasion performance of this coating compared to plasma sprayed Cr_2O_3 coatings, as previously reported, yielded very similar results for wear resistance and friction coefficient. The change in wear results is also attributed to the hardness difference [57, 58].

4. Conclusions

Taking all into consideration, our main conclusions are:

1. The coated sample and the uncoated sample were subjected to braking performance

testing under the same conditions. Differences in tribological performance of coating parameters and coating microstructure due to hard oxide ceramic structure were observed.

2. A high bonding resistance obtained by coating lamellar graphite cast iron brake disc with Cr_2O_3-2%TiO_2 ceramic composite powder by plasma spray technique were found**.**

3. The hardness of the coated disc was greatest than that of the uncoated disc and the wear rate was lower due to Cr_2O_3-2%TiO_2 powder and coating method.

4. The interface temperature of the coated disc was determined higher compared to that of the original disc. Interface temperature increased quickly due to less heat conduction of the coated disc. It is preferable that low rate of wear despite increasing temperature proved.

5. The surface roughness value was measured five times lower and good stability coefficient of friction, exhibited less wear and longer life than the those of uncoated disc.

6. In spite of the uncoated disc giving almost the same coefficient of friction value as in the coated disc, the amount of wear of the brake lining of the coated disc was lower than that of the uncoated disc and brake lining.

In this way, less emissions are left in the environment due to braking. As a result, it is thought that economic losses caused by abrasion would be also decreased.

5. References

1. Lee, Y.M; Park, J.S; Seok, C.S; Lee C.W; Kim, J.H, "Thermal stress analysis for a brake disc considering pressure distribution at a frictional surface", Proceedings of the Korean Society of Precision Engineering Conference, 842-846, 2005.

2. Hong, H; Kim, M; Lee, H; Jeong, N, "The thermo-mechanical behavior of brake discs for high-speed railway vehicles", Journal of Mechanical Science and Technology, 33(4), 1711-1721), 2019.

3. Laguna-Camacho J; Juárez-Morales, G; Calderon-Ramon C.M; Velázquez-Martínez, V; Hernández-Romero, I; Méndez-Méndez, J.V; Vite-Torres, M.A, "Study of the wear mechanisms of disk and shoe brake pads", Engineering Failure Analysis, 56, 348-359, 2015.

4. Öktem, H; Uygur İ, "Advanced friction-wear behavior of organic brake pads using a newly developed system", Tribology Transactions, 62(1), 51–61, 2019.

5. Goo, B.C," A study on the effect of parameters on the temperature distribution of brake discs", Proceedings of the Korean Society for Railway Spring Conference, 1-6, 2007.

6. Kim, J.H; Goo, B.C; Suk C.S, "A study on the temperature change of braking disc and thermal conductivity during the service", Journal of the Korea Society for Railway, 10(6), 665-669, 2007.

7. Blau, P.J. and Mc-Laughlin, J.C, "Effects of water films and sliding speed on the frictional behavior of truck disc brake material", Tribology in Industries, 36 (10), 709-715, 2003.

8. Anderson, A. E, "Friction and wear automotive brakes, ASM Handbook, Friction, Lubrication, and Wear Technology", ASM International, 2017.

9. Wu, Y; Ma, Y; Gao, W; Yang, G; Fu, H; Xi, N; Chen, H, "High temperature wear performance of laser cladding Co06 coating on high-speed train brake disc", Applied Surface Science, 481, 761-766, 2019.

10. Güney B, Mutlu İ, "Tribological properties of brake discs coated Cr_2O_3-40%TiO_2 by plasma spraying", Surface Review and Letters, 26, 10,1950075, 2019.

11. Yin, Z; Tao, S; Zhou, X; Ding, C, "Particle in-flight behavior and its influence on the microstructure and mechanical properties of plasma-sprayed Al_2O_3 coatings", Journal of the European Ceramic Society, 28, 1143-1148, 2008.

12. Ctibor, P; Píš, I; Kotlan, J; Pala, Z; Khalakhan, I; Stengl, V; Homola, P, "Microstructure and properties of plasma-sprayed mixture of Cr_2O_3 and TiO_2", Journal of Thermal Spray Technology, 22, 1163-1169, 2013.

13. Sert, Y; Toplan, N, "Tribological behavior of a plasma-sprayed Al_2O_3-TiO_2-Cr_2O_3 coating", Materials and Technology, 47, 181-183, 2013.

14. Candel, A., Gadow, R, "Optimized multiaxis robot kinematic for HVOF spray coatings on complex shaped substrates", Surface Coating Technology, 201, 2065-2071, 2006.

15. Chen, K; Song, P; Li, C; Zhou, Y; He, X; Yu, X; Lu, J, "Influence of heat treatment on

alternant-layer structure and mechanical properties of Al_2O_3-TiO_2-MgO coatings", Ceramics International, 44, 13727-13735, 2018.
16. Wang, Q; Luo, S; Shaoyi Wang, S; Wang, H; Chidambaram Seshadri Ramachandran, "Wear, erosion and corrosion resistance of HVOF-sprayed WC and Cr_3C_2 based coatings for electrolytic hard chrome replacemen"t, International Journal of Refractory Metals-Hard Materials, 81, 242-252, 2019.
17. Sathish, S; Swaminathan, C.S; Senthilvel, C; Dilip Jerold, B; Shabir, M.F; Geetha, M, "Investigation on the corrosion behavior of the bilayered ceramic coatings deposited using atmospheric plasma spraying", Procedia Technology, 12, 301-307, 2014.
18. Hegde Chitharanjan, A; Venkatakrishna, K; Eliaz, N, "Electrodeposition of Zn-Ni, Zn-Fe and Zn-Ni-Fe alloys", Surface and Coatings Technology, 205, 2031-2041, 2010.
19. Sreenivasa Rao, K.V; Ramesh, C.S; Girisha, K.G; Rakesh, Y.D, "Slurry erosive wear behavior of plasma sprayed Cr_2O_3 coatings on steel substrates", Materials Today: Proceedings, 4, 10283-10287, 2017.
20. Zamani, P; Valefi, Z, "Microstructure, phase composition and mechanical properties of plasma sprayed Al_2O_3, Cr_2O_3 and Cr_2O_3-Al_2O_3 composite coatings", Surface and Coatings Technology, 316, 138-145, 2017.
21. Chen, L.Y; Xu, T; Wang, H; Sang, P; Lu, S; Ze-Xin Wang, Z.X; Chen, S; Zhangb, L.C, "Phase interaction induced texture in a plasma sprayed-remelted NiCrBSi coating during solidification: an electron backscatter diffraction study", Surface and Coatings Technology, 358, 467-480, 2019.
22. Singh, V.P; Sil, A.R; Jayaganthan R. "Tribological behavior of plasma sprayed Cr_2O_3-3%TiO_2 coatings", Wear, 272, 149-158, 2011.
23. Babu, P.S; Sen, D; Jyothirmayi, A.; Krishna, L.R; Rao, D.S, "Influence of microstructure on the wear and corrosion behavior of detonation sprayed Cr_2O_3-Al_2O_3 and plasma sprayed Cr_2O_3 coatings", Ceramics International, 44, 2351-2357, 2018.
24. Bagde, P; Sapate, S.G; Khatirkar, R.K; Vashishtha, N; Tailor, S, "Friction and wear behaviour of plasma sprayed Cr_2O_3-TiO_2 coating", Materials Research Express, 5, 1-14, 2018.
25. Anonymous, SAE J661, Brake Lining Quality Test Procedure, Society of Automotive Engineers, Pensilvanya, USA: Standart No. SAE J661:1997.
26. https://www.oerlikon.com/metco/en/meta-navigation/search-result/?q=MaterialGuide, 15/07/ 2019.
27. Hirota, K; Takano, Y; Yoshinaka, M; Yamaguchi, O, "Fabrication and mechanical properties of almost fully-densified Cr_2O_3 ceramics", Journal of Materials Science Letters, 21 (11), 853-854, 2002.
28. Du, H.L; Datta, P.K; Burnell-Gray, J.S; Guo, X, "Influence of plasma-sprayed Mo coating on sulphidation behaviour of inconel 600 and nimonic PE11 alloys", Surface and Coatings Technology, (76-77), 1-6, 1995.
29. Hieman, R.B, "Plasma spray coating-principles and applications", VCH publishers Inc., 1996.
30. Çelik, E; Şengil, İ.A; Avcı, E, "Effect of some parameters on corrosion behaviour of plasma-sprayed coatings", Surface and Coatings Technology, 97, 355-360, 1997.
31. Anonymous, SAE J2430, "Dynamometer effectiveness characterization test forpassenger car andlight truck brake friction products. surface vehicle standard", Society of Automotive Engineers, 1999.
32. Anonymous, "How to read and understand the aftermarket standard sae j2430 / brake effectiveness evaluation Procedure-Test report", Link Testing, 1999.
33. Carlos, E.A; Ferro, E, "Technical overview of brake performance testing for original equipment and aftermarket industries in the US and europe a markets", Link Testing, 2005.
34. Miguel, J.M; Guilemany, J.M; Vizcaino, S, "Tribological study of NiCrBSi coating obtained by different processes", Tribology International, 36 (3), 181-1 87, 2003.
35. Vaclav, R; Helena, R; Dagmer, J; Peter, F; "Wear and environmental aspects of composite materials for automotive braking industry", Wear, 265, 167-175, 2005.
36. Guo, C; Zhou, J; Zhao, J; Chen, J, "Effect of ZrB_2 on the microstructure and wear resistance of Ni-based composite coating produced on pure Ti by laser cladding", Tribology Transactions, 54, 80-86, 2001.

37. Peng, L, "Preparation and tribological properties of NiCrBSiC reinforced laser alloying layer", Tribology Transactions, 56, 697-702, 20013.
38. Filip, P; Weiss, Z; Rafaja, D, "On friction layer formation in polymer matrix composite materials for brake applications", Wear, 252, 189-198, 2002.
39. Ertan, R; Yavuz, N, "Balata malzemelerinde kullanılan yapısalların balataların tribolojik ve fiziksel özelliklerine etkisi", Uludağ Üniversitesi, Mühendislik-Mimarlık Dergisi, 15, 169-177, 2010.
40. Shorowordi, K.M; Haseeb, A.S.M.A; Celis, J.P, "Velocity effects on the wear, friction and tribochemistry of aluminium MMC sliding against phenolic brake pad", Wear, 256**,** 1176-1181, 2004.
41. Bolelli, G; Cannillo, V; Lusvarghi, L; Manfredini, T, "Wear behaviour of thermally sprayed ceramic oxide coatings", Wear, 261, 1298-1315, 2006.
42. Buytoz, S; Ersöz, E; Islak, S; Orhan, N; Kurt. B; Somunkıran. İ, "Plazma püskürtme yöntemiyle oluşturulan Al_2O_3-TiO_2 kompozit kaplamaların mikro yapı karakteristikleri", International İron-Steel Symposium, 2012, Karabük, Türkiye.
43. Lee, C.H; Kim, H.K; Choi, H.S; Ahn, H.S, "Phase transformation and bond coat oxidation behavior of plasma-sprayed zirconia thermal barrier coating", Surface and Coatings Technology, 124, 1-12 2000.
44. Li, C.J; Yang, G.J; Ohmori, A, "Relationship between particle erosion and lamellar microstructure for plasma-sprayed alumina coatings", Wear, 260, 1166-1172, 2006.
45. Pawlowski, L, "The science and engineering of thermal spray coatings", John Wiley-Sons, 2008.
46. Kuroda, T; Kobayashi, A, "Adhesion characteristics of zirconia-alumina composite coatings by gastunnel type plasma spraying", Vacuum, 73, 635-641, 2004.
47. Çelik, E; Tekmen, C; Özdemir I; Çetinel, H; Karakaş, Y; Okumuş, S.C, "Effects on performance of Cr_2O_3 layers produced on Mo/cast-iron materials", Surface and Coatings Technology, (174-175), 1074-1081, 2003.
48. Luo, H; Goberman, D; Shaw, L; Gell, M, "Indentation fracture behavior of plasma sprayed nano structured Al_2O_3-%13TiO_2 coatings", Materials Science and Engineering A, 346 (1-2), 237-245, 2003.
49. Fervel, B; Normand, C; Coddet, C, "Tribological behavior of plasma sprayed Al_2O_3-based cermet coatings", Wear, 230(1), 70-77, 1999.
50. Çelik, E; Sarıkaya, Ö, "The effect on residual stresses of porosity in plasma sprayed MgO-ZrO_2 coatings for an internal combustion diesel engine", Materials Science and Engineering A, 379, 11-16. 2004.
51. Song, E.P; Ahn, J; Lee, S; Kim, N.J, "Effects of critical plasma spray parameter and spray distance on wear resistance of Al_2O_3-%8TiO_2 coatings plasma sprayed with nano powders", Surface and Coating Technology, 20, 3625-3632, 2008.
52. Eriksson, M; Bergman, F; Jacobson, S, "On the nature of tribological contact in automotive brakes", Wear, 252, 26-36, 2002.
53. Ripley, M.I; Kirstein, O, "Residual stresses in a cast iron automotive brake disc rotor", Physica, 385-386 (B), 604-606, 2006.
54. Mutlu, İ; Öner,C; Findik, F, "Boric acid effect in phenolic composites on tribological properties in brake linings", Materials and Design, 28, 480-487, 2007.
55. Zou, Z. W., Wang, Y; Zhou F.F; Wang, L; Liu, S.Y; Wang, Y. "Tribological property of plasma-sprayed Al_2O_3-13wt% TiO_2 coatings onto resin-based composites", Applied Surface Science, 431, 75-80, 2018.
56. Tyagi, R; Xiong, D.S; Li, J; Dai, J. "Elevated temperature tribological behavior of Ni-based composites containing nano-silver and hBN", Wear, 269, 884-890, 2010.
57. Fernandez, J.E; Wan, Y; Tuchoa, R; Rinconb, A. "Friction and wear behaviour of plasma-sprayed Cr_2O_3 coatings in dry sliding against AISI D2 steel", Elsevier, 1996.
58. Ahn, H.S; Kwon, O.K. "Tribological behavior of plasma-sprayed chromium oxide coating", Wear, 225-229, 814–824, 1999.
59. Wahab, J.A, Ghazali, M.J, Sajuria, Z, Otsukac, Y, Jayaprakashd, M, Nakamurae, S, Baharin, A.F.S. "Effects of micro-grooves on tribological behavior of plasma-sprayed alumina-13% titania coatings", Ceramics International, 43, 6410-6416, 2017.
60. Hawthorne, H.M, Erickson, L.C, Ross, D, Tai, H, Troczynski, T. "The microstructural

dependence of wear and indentation behavior of some plasma-sprayed alumina coatings", Wear, 203-204, 709-714, 1997.
61. Güney B, Mutlu İ, "Wear and corrosion resistance of Cr2O3%-40% TiO2 coating on gray cast-iron by plasma spray technique", Materials Research Express, 6, 096577, 2019.
62. Erdemir, A. "A review of the lubrication of ceramics with thin solid, Friction and Wear of Ceramics", Marcel Dekker, 1994.
63. Suzdal'tsev, E.I. "Fabrication of high-density quartz ceramics: research and practical aspects. Part 4. Properties of mixed quartz glass slips and preforms prepared by casting into porous molds", Refractories and Industrical Ceramics, 46 (6), 391-395, 2005.
64. Kukutschová, J; Roubíček, V; Malachová, K; Pavlíčková, Z; Holuša, R; Kubačková, J; Mička, V; MacCrimmon, D; Filip, P. "Wear mechanism in automotive brake materials, wear debris and its potential environmental impact", Wear, 267, (5-8), 807-817, 2009.